Part VII

Nebular Morphology and Dynamics

https://doi.org/10.1017/S0074180900209285 Published online by Cambridge University Press

PLANETARY NEBULAE: THEIR EVOLUTION AND ROLE IN THE UNIVERSE
IAU Symposium, Vol. 209, 2003
S. Kwok, M. Dopita, and R. Sutherland, eds.

The Correlation of PN Morphology and Parameters

Arturo Manchado[1,2]

[2]*Instituto de Astrofísica de Canarias, E-38205 La Laguna, Tenerife, Spain*
[2]*Consejo Superior de Investigaciones Científicas, CSIC*

Abstract. The morphology of a complete sample of 255 northern planetary nebulae (PNe) was studied and correlated with the nebular parameters. PNe were classified according to the following scheme: round (R, 25%), elliptical (E, 58% of the sample), and bipolar (B, 17%). Bipolars include the quadrupolar subsample. A subclass of pointsymmetric and multiple shell PNe was also found. Nine per cent of ellipticals and 46% of bipolars were found to be pointsymmetric. Thirty-five per cent of the round and 22% of the elliptical PNe were found to be multiple shell PNe (MSPNe). Galactic latitude was found to be different for each morphological class ($|b| = 8°$, $5°$ and $2°$ for types R, E, and B, respectively). Galactic height was also found to vary: $\langle z \rangle = 647$, 276, and 100 pc for categories R, E, and B, respectively. Segregation according to the chemical abundances was also found, with helium abundances of 0.10, 0.12, and 0.14 and N/O of 0.21, 0.31, and 1.33 for types R, E, and B, respectively. Both galactic distribution and chemical abundances point to a different stellar population for each morphological class, the round and bipolar types being the result of low and high stellar mass progenitor evolution, respectively.

1. Introduction

An AGB star can lose up to 80% of its mass during the last phase of thermal pulses. This envelope will eventually be ionized and a planetary nebula (PN) will form. Different mechanisms have been proposed to account for the observed morphologies. Kwok, Purton, & Fitzgerald (1978) proposed that round PNe were formed by the interaction of a low density fast wind with a high density slow wind (interacting wind model). Mellema (1995) accounted for elliptical PNe as the result of an interacting wind model with an equatorial density enhancement. Jets and ansae were explained by Frank, Balick, & Livio (1996) as the result of an accelerating fast wind interacting with a toroidal slow wind.

Different authors have proposed several explanations for the formation of bipolar PNe; Soker (1997) proposed that bipolar morphology was the result of the interaction of a close binary system that has avoided the common envelope phase. Alternatively, García-Segura, Langer, & Rózyczka (1999) proposed that a magnetic field could lead to the formation of bipolar PNe.

Pointsymmetric structures were explained by García-Segura & López (2000) as the result of a combination of a magnetic field and precession.

The formation of multiple shells in PNe (MSPNe) has been studied by following the mass loss rates during the AGB, using numerical models. Steffen & Schönberner (2000) explained MSPNe formation as the result of the mass loss experienced during the last phase of the AGB evolution. However, the grid sizes they used were too small: neither the full mass-loss process process experienced by the star, nor the influence of the ISM could be taken into account. Villaver, García-Segura, & Manchado (2002) used larger grids and found that large shells (up to 2.5 pc) are formed due to the mass loss during the AGB. Moreover, they demonstrated the importance of the ISM since a huge amount of material swept up by the wind is present in the outer shells of MSPNe.

2. On the Morphology

Many studies on the morphology of PN have been made over the past century, but most of them have suffered from strong selection effects that makes obtaining sound conclusions difficult. Pioneering work was done by Curtis (1918), who discovered large structures or "halos" around PNe. Greig (1971) divided the morphology of PN into "binebulous" and "centric" nebulae. Zuckerman & Aller (1986) studied a sample of 108 PNe and classified their morphology into bipolar, round, disk-like, and annular. Balick (1987) divided the morphological classes into round, elliptical, and butterfly, proposing an evolutionary path of "early", "middle", and "late" PNe for each.

Multiple shell PNe were studied by Chu, Jacoby, & Arendt (1987), who found that 50% of PNe were MSPNe.

Schwarz, Corradi, & Melnik (1992) studied 250 PNe and divided the different classes into stellar, elliptical, bipolar, pointsymmetric, and irregular. From a study of this sample, Stanghellini, Corradi, & Schwarz (1993) found that the central star mass distribution differs for bipolar and elliptical, and that the latter are younger and more luminous than MPSNe; Corradi & Schwarz (1995) found that elliptical have a higher galactic plane altitude ($\langle z \rangle = 320$ pc) than bipolar ($\langle z \rangle = 130$ pc) and that bipolar have an overabundance helium, nitrogen, and neon; they also found that these PNe had giant dimensions.

Manchado *et al.* (1996) studied a complete sample of 243 PNe and classified their morphology as round, bipolar, elliptical, quadrupolar, and pointsymmetric.

Górny, Stasinska, & Tylenda (1997) studied a sample of 125 PNe and found that bipolar have a higher mass, smaller z, and a higher N/O ratio, and that pointsymmetric were a separate class with $\langle z \rangle = 800$ pc. Górny *et al.* (1999) studied an additional sample of 101 PNe.

Recently this work was extended to the Magellanic Clouds: Shaw et *al.* (2000) studied a sample of 29 PNe, and found 17% to be elliptical, 29% round, 51% bipolar, and 3% pointsymmetric. The high percentage of bipolar is particularly remarkable as it is far higher than the number found in the Galaxy and could be caused by selection effects.

https://doi.org/10.1017/S0074180900209285 Published online by Cambridge University Press

3. Statistics

In order to have a homogeneous and complete data set, we have defined a complete sample of PNe whose morphological class can be correlated with their nebular parameters. This will allow us to establish a sound correlation.

3.1. Sample selection

All the members of the sample were northern PNe ($\delta > -11°$) from the Acker *et al.* (1992) catalogue with diameters greater than 4 arcsec and for which narrow band Hα , [N *II*], and [O *III*] images are available.

These criteria were fulfilled by 255 PNe: 213 from the Manchado *et al.* (1996) catalogue, 20 from Balick (1987), and 22 from Schwarz *et al.* (1992).

4. Classification scheme

The classification scheme was made taking into account the fact that each morphological class must have a minimum statistical weight. Therefore, due to the small percentage of quadrupolar PNe (3%) in the sample, the bipolar and quadrupolar class are grouped together. In addition, pointsymmetry is treated as a subclass rather than as a class. Pointsymmetric structures are present in both elliptical and bipolar PNe. Thus, the three major classes are round (R), with axial ratios of less than 1.06, elliptical (E), and bipolar (B). Types R and E also have multiple shell subclasses (MSPNe). Types E and B have pointsymmetric subclasses. Figure 1 shows an example of each of the different morphological classes. There are 63 (25%) type R, 149 (58%) type E, and 43 (17%) type B PNe.

5. Database

Statistical distances were taken from Cahn, Kaler, & Stanghellini (1992); emission lines intensities from, Kaler, Shaw, & Browning (1997) and Guerrero (1995); the other parameters were taken from Acker *et al.* (1992) and the NASA Astrophysics Data System.

6. Chemical abundances

Chemical abundances (He, N, O, Ne, and Ar) for all the PNe with available intensity lines, taken from Kaler *et al.* (1997) and Guerrero (1995), were re-calculated to avoid any methodological bias. Plasma diagnostic and ionic chemical abundances were calculated using the nebular analysis package in IRAF/STSDAS developed by Shaw *et al.* (1998). Helium abundances were derived taking collisional effects (e.g., Clegg 1987) into account. Ionization correction factors taken from Kingsburgh & Barlow (1994) were used in order to calculate elemental abundances.

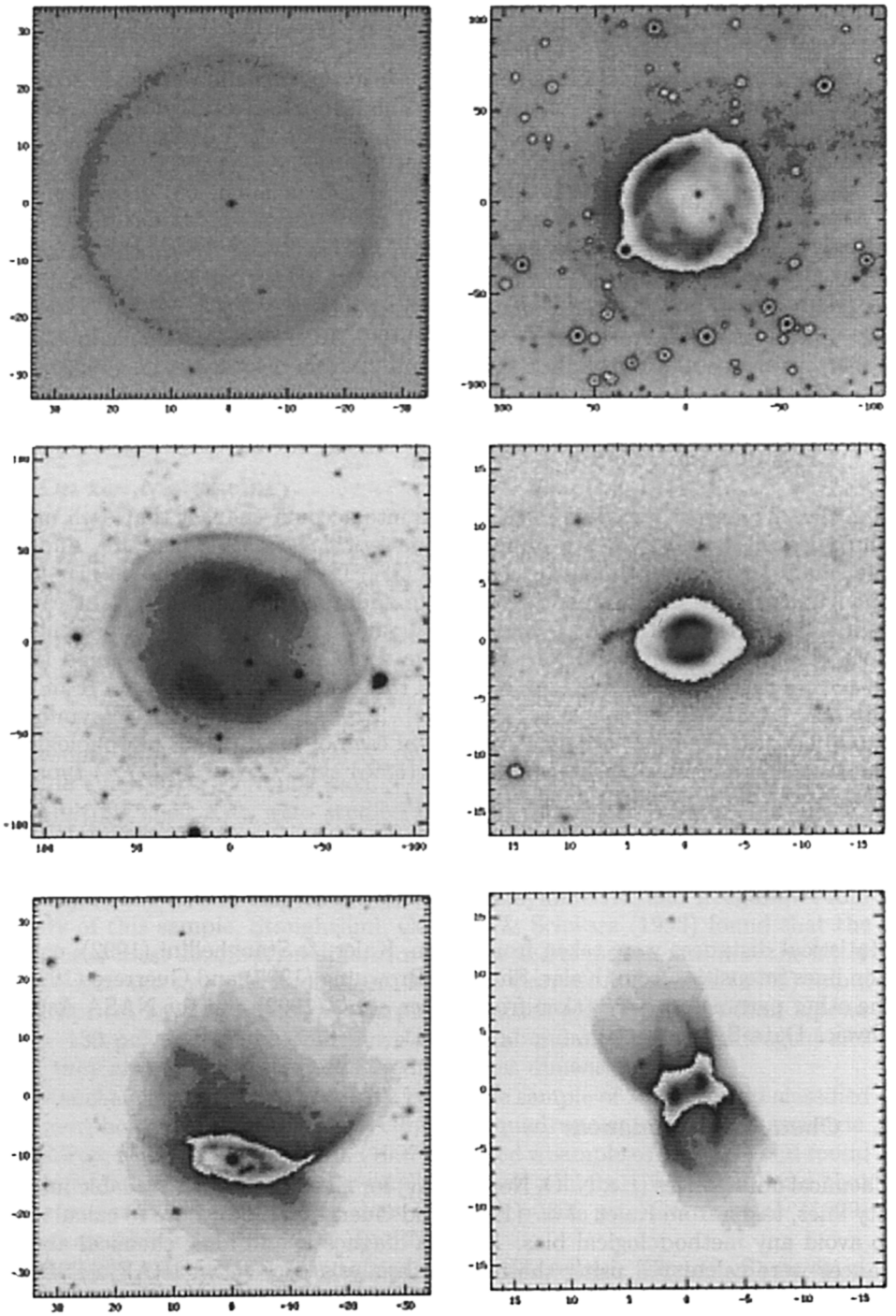

Figure 1. From left to right, top to bottom: narrow band images of the PNe A 39, NGC 2438, IC 1295, He 2-429, He 2-428 and M 2-46.

https://doi.org/10.1017/S0074180900209285 Published online by Cambridge University Press

7. Projection effects

The effect of projection must be taken into account when extrapolating the two-dimensional information for the PN images to a three-dimensional morphology. These effects are illustrated in Figure 2, where projected shapes are shown for a prolate ellipsoid, with axial ratio 1.5:1:1, and a B-type PN at different inclination angles with respect to the line of sight. Note that at angle 0°, both PNe look round. In order to find out the degree to which E- and B-type PNe could be confused with R-type PNe, we have studied the probability of mistaking one of these PNe as R. The contribution of B is negligible because of the low number (43) of these types in the sample; however, as most of the PNe (149) are E types, this may imply that a considerable number of R-type PNe could actually be E types seen pole on.

The probability of perceiving an E type as a R type depends on the axial ratio, the inclination angle, the size, and the spatial resolution. According to the average size of R types and our spatial resolution, we have classified R types as having axial ratios $a/b < 1.06$.

If it is assumed that E types are prolate ellipsoids with an axial ratio of $c : 1 : 1$, they will project an ellipse over the plane perpendicular to the line of sight. The axial ratio of this ellipse is

$$x = a/b = \sqrt{c^2 \times \sin^2(i) + \cos^2(i)}$$

where i is the projection angle. To estimate the probability of this ellipse having values $x < 1.06$, we have to know c. By analyzing the histogram of the axial ratios of E types, it is clear that $1.2 < c < 1.5$, so a probability function can be worked out. The result is 7.3% of E types could be classified as R types; therefore, 11 of the 149 E types might actually be seen as R types, which means that 17% of the R types (63) may well be E types.

8. Morphological classes

First the main classes R, E, and B are analyzed. From the whole sample, there are 63 (25%) R types, 149 (58%) E types, and 43 (17%) B types. If projection effects are taken into account the percentages will be 20% R types, 63% E types, and 17% B types. However, the sample is limited in surface brightness for the R types, as their distance histogram has a cut-off for values higher than 6.5 kpc. Therefore, if the sample is limited to distances of less than 6.5 kpc, the statistics are as follows: 36 (26%) R types, 84 (62%) E types, and 16 (12%) B types. If projection effects are taken into account these percentages will be 22% (R types), 66% (E types), and 12% (B types).

Regarding the MSPNe, 22 are R types (35% of all R), while 33 are E types (22% of all E). However, for distances of less than 6 kpc, 11 are R types (31%) and 21 are E types (26%).

With respect to the other subclass (pointsymmetric), 14 are E types (9%), while 20 are B types (46%).

https://doi.org/10.1017/S0074180900209285 Published online by Cambridge University Press

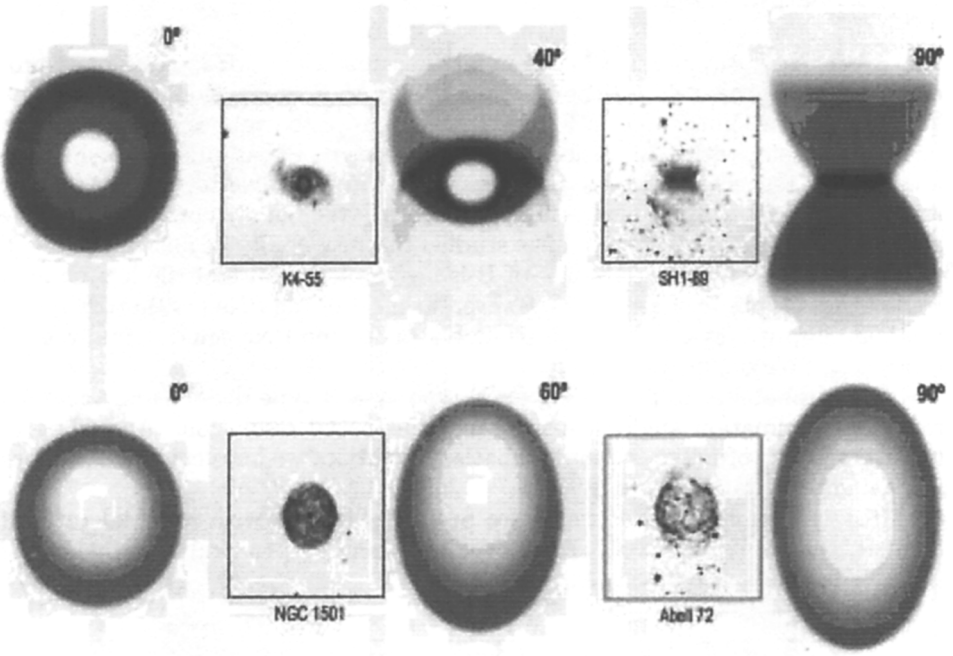

(lower) PNe at different position angles. A comparison with observed morphologies of K4-55 SH 1-89, NGC 1501 and A 72 is also shown.

9. Correlation with nebular parameters

Median values for the electronic density were found to be 400 cm^{-3} for R types, 1500 cm^{-3} for E types, and 1000 cm^{-3} for B types. R types have smaller values owing to the lower surface brightness, while the high value in B types can be explained because the brightest part of the nebula is the ring around the central star, with higher density than the lobes.

From the IRAS fluxes, dust temperatures of 82 K for R and E types, and 69 K for B types were found.

The median values of helium abundances for classes R, E, and B are 0.102, 0.121 and 0.136, respectively. This is consistent with classes R and E being type II PNe and class B being type I PNe (Torres-Peimbert & Peimbert 1997).

The median values of the N/O ratios for classes R, E, and B are 0.21, 0.30, and 1.33, respectively. This is again consistent with classes R and E being type II PNe and class B being type I PNe.

The median values for the diameters are 25.0, 24.5 and 24.5 arcseconds for classes R, E, and B, respectively. If the statistical distances are used, the diameters are 0.50, 0.36, and 0.50 pc for classes R, E, and B, respectively.

The median values for the absolute value of the Galactic latitude $|b|$ is 7.8°, 4.9°, and 2.3° for classes R, E, and B, respectively.

https://doi.org/10.1017/S0074180900209285 Published online by Cambridge University Press

Using the statistical distances, the median values of the Galactic heights $\langle z \rangle$ were found to be 647, 276, and 100 pc for classes R, E, and B, respectively. This implies progenitor masses higher for class B than for classes E and R.

In order to find out whether a segregation between the pointsymmetric subclass exists, the median values of $\langle z \rangle$ were also investigated and were found to be 308 pc for class E and 310 pc for class E with pointsymmetric structure. Therefore, pointsymmetry in class E does not depend on the mass of the progenitor. However, the values were 110 pc for class B and 248 pc for class B with pointsymmetry, implying different progenitor masses for bipolars and bipolars with a pointsymmetric structure (the latter being less massive).

This is consistent with the scenario of García-Segura *et al.* (2000), who propose two different mass distributions in the formation of bipolar PNe. Single high mass stars will form bipolar PNe due to rotation, while binary systems will form bipolar PNe with a pointsymmetric structure.

Finally, the He and N/O abundances, together with their Galactic distribution, imply that bipolar PNe have high stellar mass progenitors, while elliptical and round PNe have different mass progenitors.

10. Future work

The data set for parameters should be completed. There are many PNe with no data for their chemical abundances, expansion velocities, or central star parameters.

With space platforms such as HST and NGST this study could be extended to nearby galaxies (e.g., the LMC and M31).

Acknowledgments. I would like to thank Letizia Stanghellini, Eva Villaver, and Martín Guerrero for their contributions. This research was made possible partly by grant PB97-14335-C02-01 from the Spanish Dirección General de Enseñanza Superior.

References

Acker, A., Ochsenbein, F., Stenholm, B., Tylenda, R., Marcout, J., Schohn, C. 1992, Strasbourg-ESO catalogue of Galactic planetary nebulae, ed. ESO

Balick , B. 1987, AJ 94, 671

Cahn, J.H., Kaler, J.B., & Stanghellini, L. 1992, AAS 94, 399

Chu, Y. -H., Jacoby, G. H., & Arendt, R. 1987, ApJS 64, 529

Clegg, R.E.S. 1987, MNRAS, 229,31

Corradi, R. L. M & Schwarz, H. E. 1995, A&A 293, 871

Curtis, H.D. 1918, Pub. Lick Obs. 13, 57

Frank, A., Balick, B., & Livio, M. 1996 ApJ, 471, L53

García-Segura, G., Langer, N., & Rózyczka, M. 1999 ApJ, 517, 767

García-Segura, G. & López, J.A. 2000 ApJ, 544, 336

García-Segura, G., Franco, J., López, J.A., Langer, N., & Rózyczka, M 2000, RMexAC, 9, p.210

Górny, S.K., Stasinska, G., & Tylenda, R. 1997, A&A 318, 256

Górny, S.K., Schwarz, H.E., Corradi, R.L.M., & Winckel, H. van 1999, A&AS 136, 145

Greig , W. E., 1971, A&A 10, 161

Guerrero, M.A. 1995, PhD Thesis, Univ. La Laguna

Kaler, J.B., Shaw, R.A., & Browning, L. 1997, PASP 109, 289

Kingsburgh, R.L. & Barlow M.J. 1994, MNRAS, 271, 257

Kwok, S., Purton, C.R., & Fitzgerald, P.M. 1978, ApJ 219, 17

Manchado, A., Guerrero, M.A., Stanghellini, L., & Serra-Ricart, M. 1996, The IAC Morphological Catalog of Northern Galactic PNe, ed. IAC http://www.iac.es/nebula/nebula.html

Mellema, G. 1995, "Asymmetrical PN", ed. Harpaz, p. 229

NASA Astrophysics Data System; http://adsabs.harvard.edu/

Schwarz, H. E., Corradi, R. L. M., & Melnik J. 1992, A&AS 96, 23

Shaw, R.A., De La Peña, M.D., Katsanis, R.M., & Williams R.E. 1998, Astronomical Data Analysis Software and Systems VII ASP Conference Series, Vol. 145, 192 eds. R. Albrecht, R. N. Hook and H. A. Bushouse

Shaw, R.A, Stanghellini, L., Mutchler, M., Balick, B., & Blades, J.C. 2000, ApJ, 548, 727

Soker, 1997, ApJS, 112, 487

Stanghellini, L., Corradi, R. L. M, & Schwarz, H. E, 1993 A&A 279, 521

Steffen, M. & Schönberner, D. 2000, A&A, 357, 180

Torres-Peimbert, S., & Peimbert, M. 1997, IAU Symp 180, p. 175, eds. H. J. Habing and H. J. G. L. M. Lamers.

Villaver, E., García-Segura, G., & Manchado, A. 2002, ApJ, 571, 1

Zuckerman, B. & Aller, L. H. 1986, ApJ 301, 772

Xiao Wei Liu at the nature preserve (photo courtesy of R. Rubin).

https://doi.org/10.1017/S0074180900209285 Published online by Cambridge University Press